Stochasticity and bistability in horizontal transfer control of a genomic island in *Pseudomonas*

Marco Minoia, Muriel Gaillard, Friedrich Reinhard, Milos Stojanov, Vladimir Sentchilo, and Jan Roelof van der Meer[1]

Department of Fundamental Microbiology, University of Lausanne, 1015 Lausanne, Switzerland

Edited by Richard P. Novick, New York University School of Medicine, New York, New York, and approved November 12, 2008 (received for review June 26, 2008)

Genomic islands (GEI) comprise a recently recognized large family of potentially mobile DNA elements and play an important role in the rapid differentiation and adaptation of bacteria. Most importantly, GEIs have been implicated in the acquisition of virulence factors, antibiotic resistances or toxic compound metabolism. Despite detailed information on coding capacities of GEIs, little is known about the regulatory decisions in individual cells controlling GEI transfer. Here, we show how self-transfer of ICE*clc*, a GEI in *Pseudomonas knackmussii* B13 is controlled by a series of stochastic processes, the result of which is that only a few percent of cells in a population will excise ICE*clc* and launch transfer. Stochastic processes have been implicated before in producing bistable phenotypic transitions, such as sporulation and competence development, but never before in horizontal gene transfer (HGT). Bistability is instigated during stationary phase at the level of expression of an activator protein InrR that lays encoded on ICE*clc*, and then faithfully propagated to a bistable expression of the IntB13 integrase, the enzyme responsible for excision and integration of the ICE*clc*. Our results demonstrate how GEI of a very widespread family are likely to control their transfer rates. Furthermore, they help to explain why HGT is typically confined to few members within a population of cells. The finding that, despite apparent stochasticity, HGT rates can be modulated by external environmental conditions provides an explanation as to why selective conditions can promote DNA exchange.

integrase | integrative and conjugative element | regulation | 3-chlorobenzoate | clc element

Horizontal gene transfer (HGT), the exchange of DNA between species other than by vertical descent, is of major importance for prokaryotic evolution (1, 2). Various mechanisms play a role in DNA exchange, most commonly known as conjugation, transformation and phage transduction (3). Most pertinently, HGT is responsible for the rapid adaptation of bacteria to acquire new virulence factors and antibiotic resistances or to metabolize toxic compounds (4). Genomic islands (GEIs) are the most recent addition to the suite of known mobile DNA elements in prokaryotes. Large-scale prokaryotic genome sequencing efforts have revealed a wide diversity and abundance of GEIs, suggesting ancient origins and multiple families of different GEI-types (5–13). Like other mobile DNA, GEIs contribute to bacterial survival, differentiation, and adaptation in particular niches by providing, e.g., virulence factors (7, 14, 15), host-cell adhesion (16), iron uptake (17, 18), antibiotic resistance (19, 20), toxin production (10), aromatic compound metabolism (21, 22), or plant symbiosis (23). Because of their wide distribution, GEI form an important model to test various hypotheses on HGT in general. One of the key questions that have escaped much attention concerns the regulatory decisions controlling HGT at the level of the individual bacterial cell. This seems surprising given the typical low frequencies (1% or less) for HGT in bacterial populations (24), and suggests that cells, despite their clonality, are undergoing some sort of phenotypic variation into transfer-proficient and transfer-silent subpopulations. The phenomenon of phenotypic bifurcation in clonal bacterial populations, or "bistability," is well-known from competence development and sporulation in *Bacillus subtilis* (25, 26), but has not before been implicated in HGT.

GEI have an intricate life-style of their own, which can be concluded from detailed studies on a number of elements, such as SXT of *Vibrio cholerae* (27), ICE*Hin*1056 of *Haemophilus influenzae* (20, 28), SaPI from *Staphylococcus aureus* (15), and PAPI-1 from *Pseudomonas aeruginosa* (29). Similar to prophages but in contrast to plasmids, GEIs are normally integrated in the host's chromosome. At low frequencies they can excise (27, 29–31), and transfer to a new cell either by cotransduction (15) or by conjugation (28). The GEI can subsequently reintegrate via site-specific recombination mediated by the integrase, usually at one or more specific target sites in the chromosome (30, 32). Not all GEI detected by sequencing have a "complete" life-style but may lack one or more functional aspects, which has been interpreted as evolutionary regression (2). Those GEI that are capable of excision, conjugative transfer, and integration have been grouped with other mobile DNA, such as conjugative transposons as integrative and conjugative elements (or ICEs) (33).

The model for HGT we study here is the *clc* element (designated as ICE*clc*) (21). ICE*clc* is a 103-kb self-transferable GEI first described in *Pseudomonas knackmussi* strain B13, where it is present in two copies (34). The most prominent phenotype encoded by ICE*clc* is the capacity conferred on the host to use the aromatic compounds 3-chlorobenzoate and 2-aminophenol as unique carbon and energy substrates. ICE*clc* is a representative of a large set of syntenic GEIs present in *Gamma-* and *Betaproteobacteria* (20, 21, 28) (Fig. S1). The process of ICE*clc* self-transfer begins with activation of the promoter of the *intB13* integrase gene (P_{int}), which is located downstream of the $tRNA^{Gly}$ integration site (31, 35), leading to an excised and covalently closed ICE*clc* molecule (Fig. S2). The excised ICE*clc* molecule is supposed to self-transfer via a GEI-type IV secretion system in analogy to ICE*Hin*1056 for which this mechanism was recently discovered (28). In the new host cell, ICE*clc* site-specifically recombines with the 3′ 18-bp of a $tRNA^{Gly}$ gene, leading to integration of the element in the host's chromosome and restoration of the $tRNA^{Gly}$ gene. Site-specific recombination is catalyzed by the IntB13 integrase, which may be temporarily overexpressed from the strong constitutive promoter in the excised ICE*clc* molecule (32, 35). Putative regulatory elements implicated in *intB13* expression in the integrated ICE*clc* have been located at the ICE*clc*'s end opposite to the *intB13* position (35).

Author contributions: J.R.v.d.M. designed research; M.M., M.G., M.S., and V.S. performed research; M.M., M.G., F.R., V.S., and J.R.v.d.M. analyzed data; and M.M. and J.R.v.d.M. wrote the paper.

The authors declare no conflict of interest.

This article is a PNAS Direct Submission.

Freely available online through the PNAS open access option.

[1]To whom correspondence should be addressed. E-mail: janroelof.vandermeer@unil.ch.

This article contains supporting information online at www.pnas.org/cgi/content/full/0806164106/DCSupplemental.

One of those was a gene named *inrR* (i.e., integrase regulator) (Fig. S2). Here, we demonstrate that InrR is positively controlling *intB13* expression, and, therewith, ICE*clc* excision and transfer. Single-cell reporter gene studies showed that expression of both *intB13* and of *inrR* is limited to a small subpopulation of cells, typical for bistability.

Results

***P. knackmussi* Strains with Deletions in *inrR* Are Impaired in ICE*clc* Activation.** A 156-bp in-frame deletion of one or both *inrR* genes in either of the ICE*clc* copies on the chromosome of *Pseudomonas knackmussii* strain B13 was generated by double homologous recombination and marker exchange to avoid any polar effects on downstream located genes (Fig. S3 and *SI Text*). Various effects were observed in B13 strains with the *inrR* in frame deletion that were consistent with a decrease or loss of ICE*clc* mobility. First, the frequency of ICE*clc* transfer from strain B13 as the donor to *Pseudomonas putida* UWC1 as the recipient decreased from $1.4 \pm 0.2 \times 10^{-2}$ transconjugants per recipient after 48 h for wild-type B13 to up to 2 orders of magnitude when *inrR* was deleted (Fig. 1*A*). Double *inrR* deletions produced fewer transconjugants (e.g., $3.1 \pm 0.2 \times 10^{-4}$ after 48 h) than the single deletion ($1.4 \pm 0.2 \times 10^{-3}$), suggesting partial complementation of transfer by one of the copies. Second, the amount of excised ICE*clc* DNA was reduced in populations of single and double *inrR* deletion mutants, with the double mutant being more severely affected than the single deletion (Fig. 1*B*). As the excised form is a prerequisite for subsequent transfer, reduced transfer rates, and decreased amounts of the ICE*clc* excised form are in agreement. Third, expression from the *intB13* integrase gene in individual cells was significantly reduced in the *inrR* mutants. This was inferred from measurements of enhanced green fluorescent protein (egfp) expression in individual cells of strain B13 and the *inrR* mutants, equipped with a single copy chromosomal transcriptional fusion of the *egfp* gene to the P_{int} promoter (Fig. 1*C*, 2*A*). These results, therefore, were all in agreement and led us to conclude that InrR is implicated in activation (or derepression) of *intB13* expression. Contrary to our expectations, purified N-terminal His_6-tagged InrR did not detectably bind DNA fragments comprising the P_{int} promoter region between the integration site (*attR*) and the start of the *intB13* gene in electrophoretic mobility assays (data not shown). Although we cannot exclude that N-terminal His_6-tagged InrR is folded differently as wild-type InrR, the absence of detectable DNA binding to the P_{int} promoter suggests that the mode of action of InrR is not that of a classical transcription activator.

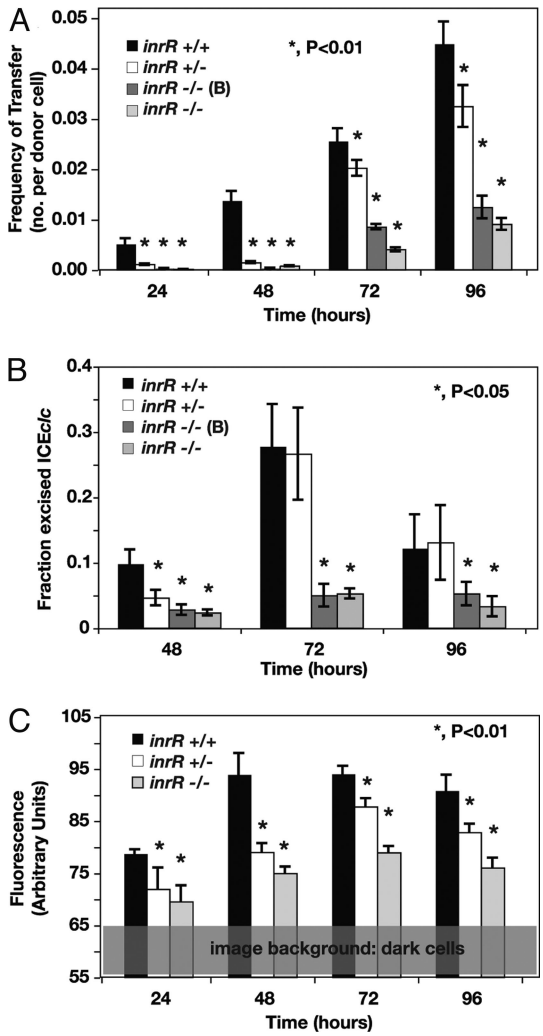

Fig. 1. Effects of *inrR* deletions on ICE*clc* behavior. (*A*) Transfer frequencies of ICE*clc* from *P. knackmussii* strain B13 or one of the *inrR* deletion mutants to *P. putida* UWC1 as recipient. (*B*) Fraction of the ICE*clc* excised form per integrated copy in cultures grown with 3-chlorobenzoate minimal medium at different incubation time points. (*C*) 95% percentile of the cumulative distribution of fluorescence values of individual cells in cultures grown with 3-chlorobenzoate medium. Time 24 h corresponds to the beginning of stationary phase.

Bistable Expression of *intB13* and *inrR*. *P. knackmussii* B13 cells with a single-copy P_{int}-*egfp* fusion did not produce egfp expression detectable with epifluorescence microscopy during exponential phase. Interestingly, in stationary phase ≈3% of cells within a population displayed egfp-specific fluorescence (Figs. 2*A* and 3*A*). This proportion was significantly higher when cells were grown with 3-chlorobenzoate than with fructose or glucose (Fig. 3*A*). These results indicated that *intB13* was expressed in a bistable manner and that, most likely, ICE*clc* became excised only in those cells.

To further understand the bistable nature of *intB13* gene expression, we focused on *inrR* expression itself. Reverse transcriptase-PCR analysis of total RNA from wild-type strain B13 grown with 3-chlorobenzoate revealed that *inrR* is the second gene in a 4-gene operon (Fig. 4*A*). The transcriptional start site was located upstream of the gene ORF95213 (Fig. 4*B*). The sequence in this area showed clear features for a stationary phase expressed promoter (Fig. 4*C*), which we named P_{inR}. Consequently, it seemed likely that *inrR* expression would be controlled by an RpoS-like sigma factor and take place primarily in stationary phase. Transcriptional gene fusions between the P_{inR} promoter and the *egfp* gene were constructed and inserted in single copy in *P. knackmussii* B13. Single-cell epifluorescence analysis demonstrated that the P_{inR} promoter indeed became active during early stationary phase and not during exponential growth (Fig. 2*B*). Egfp expression from P_{inR} was not significantly different in the single or the double *inrR* deletion mutant of strain B13, indicating that InrR does not autoregulate its own expression (Table S1). Most strikingly, however, and similar to B13 cells carrying a single-copy P_{int}-*egfp* fusion, only a small proportion of cells in the population expressed egfp under the control of P_{inR} (Fig. 2*B*). This proportion was again significantly higher when cells were grown with 3-chlorobenzoate than with fructose or glucose (Fig. 3*A*).

Colocalization of Bistable *inrR and intB13* Expression. We then asked the question whether the reason for bistability at the P_{int} promoter was in fact a consequence of bistable expression at the P_{inR} promoter. A further derivative of strain B13 was created in

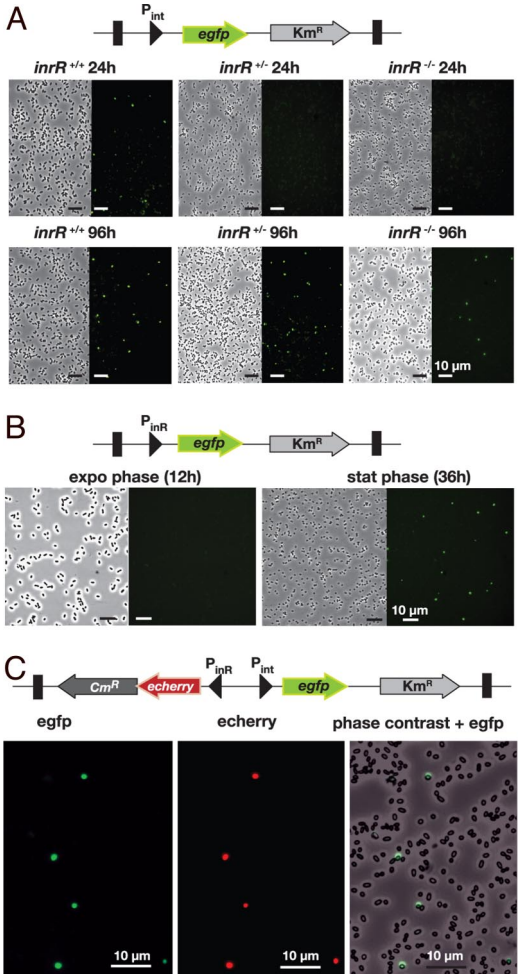

Fig. 2. Stochastic expression of the P_{int} and P_{inR} promoters in *P. knackmussii* strain B13 cultures from single copy chromosomal transcriptional fusions to the *egfp* and/or *echerry* gene. (*A*) Egfp expression from P_{int} in strain B13 or the single and double *inrR* deletion derivatives. (*B*) *P. knackmussii* strain B13 cells equipped with single copy P_{inR}-*egfp*. (*C*) Colocalization of echerry and egfp fluorescence in stationary phase cells (28 h) of *P. knackmussii* strain B13 with a single copy P_{int}-*egfp*, P_{inR}-*echerry* fusion. Shown are phase-contrast micrographs at 1,000× magnification and corresponding epifluorescence images for egfp or echerry.

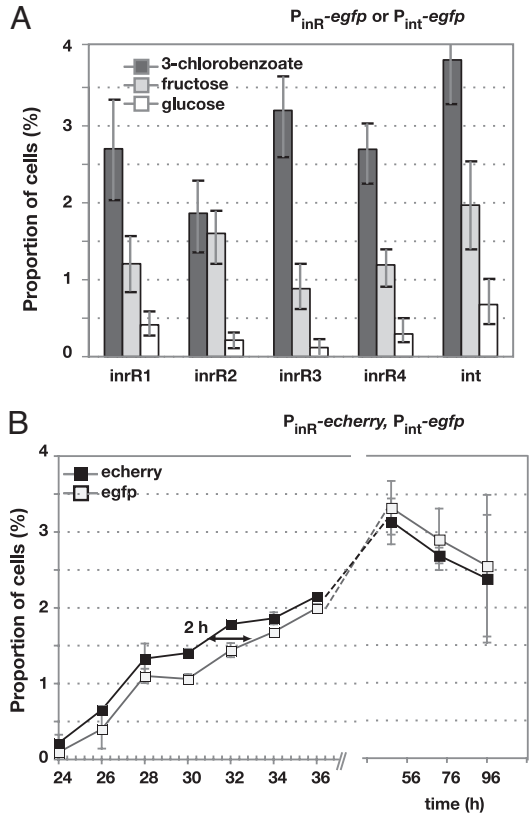

Fig. 3. Bistable stochastic expression of egfp and/or echerry from P_{inR} or P_{int} in *P. knackmussii* strain B13. (*A*) Subpopulation sizes expressing egfp from P_{inR} (four randomly picked clones with different chromosomal insertion site of the reporter gene fusions) or P_{int} in stationary phase (76 h) after growth on different carbon substrates. Error bars denote calculated 95% confidence intervals on the subpopulation size. (*B*) Bistable echerry expression from P_{inR} preceeds that of egfp from P_{int} in *P. knackmussii* cells by ≈ 2 h (see Table 1).

which egfp was produced from P_{int} and echerry from P_{inR}, both on the same minitransposon and inserted in single copy (Fig. 2*C*). These two autofluorescent proteins have emission spectra that are sufficiently well separated to not interfere with one another even at low expression levels (36). Indeed, in stationary phase cultures grown with 3-chlorobenzoate, echerry colocalized with egfp in the same cell. This indicates that cells that express *inrR* also express *intB13* (Fig. 2*C*). These cells, most likely, are the ones, which will activate ICE*clc* excision and continue to transfer should a suitable recipient be present. In fact, the proportion of cells expressing egfp from P_{int} in stationary phase (3–5%) equals the maximum transfer frequency observed for ICE*clc* ($\approx 4 \times 10^{-2}$ per donor, Fig. 1*A*), suggesting that all such cells engage in successful transfer when presented with a suitable recipient cell.

Echerry and egfp measurements of individual cells cultured with 3-chlorobenzoate in minimal medium further showed that echerry formation preceded egfp by ≈2 h (Fig. 3*B* and Table 1). To avoid that slight differences in maturation rate of egfp and echerry (36) would be responsible for this time effect, we repeated the experiment with a strain in which the promoter-reporter gene fusions were reversed. In this case, the egfp fluorescence (now controlled by P_{inR}) appeared first (Fig. S4 and Table 1), followed in the same cell by echerry (expressed from P_{int}). This strongly suggests, therefore, that the P_{inR} promoter (and thus *inrR*) is expressed first, after which InrR could promote expression from P_{int} (and thus *intB13*). Because at this point they are in stationary phase, the cells do not further divide and any egfp or echerry measured is the result of expression in those particular cells and not of inheritance by cell division. Because close to 100% of all individual cells that express echerry (from P_{inR}) also express egfp (from P_{int}) in stationary phase, this would mean that a robust bistable signal propagation is generated (Table 1).

Discussion

We are unaware of another study describing bistable control of GEI-transfer or HGT in general. Our results suggest a series of stochastic events underlying bistability formation. The first detected event occurs at the level of *inrR* expression, bifurcating the population in cells that produce InrR or not. Bistability dictates that (small) cell-to-cell stochastic expression differences (here in *inrR*) would be amplified and temporarily locked; something, which can be achieved by mechanisms such as a positive or a double-negative transcriptional feedback loop (37). The nature of this amplification mechanism at the level of P_{inR} is currently not clear, but may be less in amplitude than, e.g., the ComK-*comKp* autoregulatory loop, because only 3% of all cells

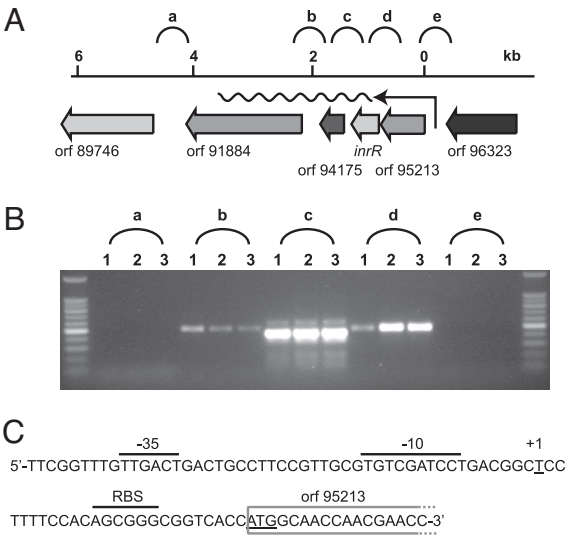

Fig. 4. Operon structure and transcription start site determination for the *inrR* transcript. (*A*) Gene localization and direction of the 4-gene operon containing *inrR*. (*B*) RT-PCR products with primers targeting regions *a*-*e* indicated in *a* from total RNA isolated from *P. knackmussii* strain B13 grown with 3-chlorobenzoate in stationary phase (Table S2). (*C*) Sequence of the region upstream of ORF95213 and indication of the 5′-end of the transcript (as ″+1″). Corresponding −10 and −35 regions and the ribosome binding site (RBS) are overligned. Note the extended −10 TG motif typical for σ^s promoters (39).

engage in InrR-IntB13 bistability [compared with ≈20% for competence (25)]. Because *inrR* mutants still showed bistable egfp expression from P_{inR} we conclude it is unlikely that InrR itself is provoking feedback transcription amplification, although it might somehow influence its own activity. The "locked" state of the bistability is apparent from the results that cells in which *inrR* is expressed propagate bistable expression at *intB13*. However, because previous results indicated the implication of a repressor on *intB13* expression (35), we postulate that the control of P_{int} actually comprises a second mechanism for bistable control, involving a balance between two counteracting factors (Fig. S5). Cells that have a high amount of InrR would be able to tip the balance in favour of activation at the P_{int} promoter, whereas cells expressing InrR at very low amounts would repress P_{int}. Because InrR does not seem to act as a classical DNA binding protein, it may impose its function by direct protein–protein interaction on the presumed transcriptional repressor for *intB13* expression (Fig. S5). Not only are the population proportions and individual cells expressing *inrR* (seen with P_{inR}-*egfp* or -*echerry* fusions) the same as those expressing *intB13*, but both increase after growth with 3-chlorobenzoate compared with fructose or glucose (Fig. 3*A*). This indicates that the bistable switch is stochastic but can be modulated by external conditions.

The InrR control mode might actually be a much more common mechanism. For example, currently >60 orthologous members of InrR exist in GenBank (Fig. S6), most of which have been detected in putative GEI-regions of bacterial genomes. Furthermore, the large number of genome regions highly related to the functional core of ICE*clc* (Fig. S1), as recognized in ref. 20, is a strong indication that the bistable regulation mode for ICE*clc* transfer might be a rather common way for GEIs of this family to decide on excision and transfer. In addition, even though this was not looked at specifically with the help of single-cell reporter gene fusions, the behavior of other GEI-types suggests bistable control mechanisms as well. For example, excision and transfer of SXT of *V. cholerae* is controlled by a repressor-activator loop similar as for phage Lambda, which has been predicted to produce bistability (37). This loop implicates SetR, a repressor that undergoes RecA-dependent cleavage during SOS-response, upon which the transcription factors SetC and SetD can activate expression of the integrase and transfer genes (27). Interestingly, SOS activation leads to an increase of SXT transfer from *Escherichia coli* from ≈10^{-4} to 10^{-2} per donor (27), which is in the same order of frequency as observed for ICE*clc*. Also ICE*Ml*Sym^{R7A} from *M. loti* excises at a maximum frequency of ≈1% in stationary phase, whereas observed transfer frequencies are in the order of 10^{-4} per donor (30). Finally, the element PAPI-1 in *P. aeruginosa* excises in a proportion of 0.16% in a population of cells in stationary phase and transfers at frequencies between 10^{-4} and 10^{-6} per donor (29). All of these results are thus in agreement with a more general hypothesis of bistable control of GEI transfer, albeit probably

Table 1. Proportion of cells expressing both P_{inR}-*echerry* and P_{int}-*egfp* or P_{inR}-*egfp* and P_{int}-*echerry* in cultures of *P. knackmussii* strain B13

	P_{inR}-*echerry*, P_{int}-*egfp*				P_{inR}-*egfp*, P_{int}-*echerry*			
Incubation time,* h	Proportion echerry†	Proportion egfp†	Percentage of common per echerry‡	Percentage of common per egfp‡	Proportion echerry†	Proportion egfp†	Percentage of common per echerry‡	Percentage of common per egfp‡
24	0.22 (±0.11)	0.09 (±0.06)	33	75	0.09 (±0.12)	0.48 (±0.28)	18	12
26	0.65 (±0.05)	0.40 (±0.26)	58	96	0.42 (±0.16)	1.1 (±0.08)	68	26
28	1.3 (±0.19)	1.1 (±0.09)	83	100	0.7 (±0.3)	1.8 (±0.2)	70	28
30	1.4 (±0.06)	1.1 (±0.07)	70	96	2.2 (±0.4)	2.9 (±0.6)	58	48
32	1.8 (±0.01)	1.4 (±0.09)	80	98	—	—	—	—
34	1.9 (±0.08)	1.7 (±0.01)	88	98	—	—	—	—
36	2.2 (±0.02)	2.0 (±0.06)	89	97	2.5 (±1.2)	3.8 (±0.8)	76	41
48	3.1 (±0.30)	3.3 (±0.36)	97	92	3.9 (±0.5)	3.9 (±0.3)	81	80
72	2.7 (±0.10)	2.9 (±0.41)	96	90	—	—	—	—
96	2.4 (±0.85)	2.5 (±0.94)	100	93	—	—	—	—

**P. knackmussii* B13 (P_{inR}-*echerry*, P_{int}-*egfp*) or (P_{inR}-*egfp*, P_{int}-*echerry*) cells cultured in batch on minimal medium with 5 mM 3-chlorobenzoate as sole carbon and energy substrate. Incubation time denotes time of sampling since inoculation start; 24 h corresponds to early stationary phase. Cell samples immediately imaged under epifluorescence microscopy at two separate wavelengths for egfp and echerry.

†Proportion of cells with fluorescence in echerry or egfp filter above background (Fig. S4 *B*-*D*) compared to total number of cells in sample ($n > 1'500$ cells). Values are average from triplicate samples of two independent *P. knackmussii* B13 (P_{inR}-*echerry*, P_{int}-*egfp*) or three (P_{inR}-*egfp*, P_{int}-*echerry*) clones (i.e., having different mini-Tn insertion positions).

‡Percentage of cells having both echerry and egfp intensities above background per number of those having echerry or egfp.

generated by different mechanisms in the case of SXT, ICE*Ml*Sym^{R7A}, PAPI-1, and ICE*clc*.

Our results explain why not all cells in a population engage in GEI transfer. Despite being seemingly "random" in a population of cells, decisions on ICE*clc* transfer appear to be governed by highly complex signaling chains within individual cells. For the time being, the most likely explanation is that the choice for ICE*clc* excision in an individual cell is stochastic. Because excision is a requirement for ICE*clc* transfer, the stochastic decision for excision forms a key event in transfer control, albeit not the sole. For instance, expression of the transfer apparatus and DNA mobilization enzymes must be simultaneously ensured. The source for stochasticity may originate in transcriptional noise at the *inr* promoter, which is amplified to bistability and then subsequently faithfully transmitted to the *intB13* promoter. At present the nature and magnitude of the noise at the *inr* promoter (e.g., intrinsic or extrinsic) could not be reliably investigated because of the low frequency of the bistable population expressing InrR and IntB13 (Fig. S4 *B–D*). We are convinced that the comprehension of such stochastic mechanisms is important for understanding the conditions favoring GEI horizontal transfer, which in the long term may provide better control over desired and undesired bacterial adaptation processes.

Materials and Methods

Bacterial Strains and Culture Conditions. Bacterial strains used in this study are described in *SI Text*. *P. knackmussii* B13 strains were cultured in liquid medium under batch conditions at 30 °C and shaking. Cultures were typically growing exponentially between 6 and 18 h after inoculation, whereas stationary phase (i.e., cessation of growth) was reached after 24 h. Increase in culture turbidity at 600 nm was followed during growth to estimate the onset of the stationary phase and exact sampling times for epifluorescence microscopy.

***ICEclc* Self-Transfer.** Self-transfer was tested by mixing donors (*P. knackmussii* B13 or one of the *inrR* deletion derivatives) and recipient (*P. putida* UWC1) on membrane filters for 24, 48, 72, or 96 h as described in ref. 38. Transconjugants (*P. putida* UWC1 with ICE*clc*) were selected on minimal medium plates with 5 mM 3-chlorobenzoate as sole carbon and energy source (to select for ICE*clc*) and 50 μg per ml rifampicin (resistance marker of the recipient). Transfer frequencies were expressed as number of transconjugant colonies per number of donors.

Mutant Construction. To produce deletions in *inrR* on either of the two ICE*clc* copies in *P. knackmussii* strain B13 we used homologous recombination with a cloned gene containing an internal deletion of 156 base-pairs produced with the PCR. The *inrR*-derivative was cloned on a nonreplicative plasmid for *Pseudomonas* (Fig. S3). Single recombinants (i.e., those in which the whole plasmid was integrated) in strain B13 were selected by resistance to tetracycline and purified. Double recombinants were enriched and plated, after which individual colonies were screened by the PCR for the appropriate integration and absence of plasmid replicon. Strangely, strain B13 with a double *inrR* mutation was not able to grow with 3-chlorobenzoate and cultures developed a strong black color as a result of photopolymerization of chlorocatechol, a metabolic intermediate from 3-chlorobenzoate. However, mutants growing with 3-chlorobenzoate developed spontaneously in the culture flasks. Purified double *inrR* mutants displayed growth rates similar as *P. knackmussii* B13 wild-type and no longer produced black color with 3-chlorobenzoate as growth substrate. *InrR* mutants are marked *inrR*$^{+/-}$ (one interrupted copy), *inrR*$^{-/-}$ (two interrupted copies) or *inrR*$^{-/-}$"B," the double *inrR* mutant strain that accumulated dark color when incubated with 3-chlorobenzoate.

Single-Copy Promoter Gene Fusions. Expression from P_{int} or P_{inrR} was measured at single-cell level by introducing a stable single-copy chromosomal transcriptional fusion via minitransposon Tn*5* delivery (35). Schematic fusion structures are depicted in Fig. 2 on top of each panel. Appropriate DNA fragments containing either P_{int} or P_{inrR} were cloned in front of promoterless *egfp* or *echerry* genes, and the fusion was subsequently inserted within the miniTn*5* delivery vector. The *echerry* gene is an *E. coli* optimized codon variant of *mcherry* (36). For colocalization studies a single miniTn5 was inserted with both P_{int}-*egfp* and P_{inR}-*echerry* or with P_{int}-*echerry* and P_{inR}-*egfp* (*SI Text*, Fig. 3*C*). Four independent clones with different insertion position of the miniTn5s were analyzed.

Fluorescence Microscopy. Culture samples of 10 μL were immediately placed on regular microscope slides, closed with a 50 mm $\times$ 0.15 mm coverslip, and imaged within 1–2 min. Fluorescence intensities of $\approx$1,000 individual cells were digitally recorded on image fields not previously exposed to UV-light to avoid bleaching. The mean pixel intensity of all objects was quantified by an automatic subroutine in the program Metaview (version 6.1; Universal Imaging; Visitron Systems) as described in ref. 31. Fluorescence intensities per cell were expressed as cellular average gray values (AGVs). Subpopulation expression was determined from the 95% percentile in a cumulative ranking of all objects according to their AGV. Bootstrapping served to calculate 95% confidence intervals on percentile determinations. Relative proportions of subpopulations were determined from the intercept between linear regressions on each of the subpopulations plotted in quantile normalized graphs of all individual cells versus their average gray value (Fig. S4 *B–D*). Images for display were autolevelled and further cropped to the final size with Adobe Photoshop.

DNA and RNA Techniques. Quantification of the ICE*clc* circular form in cultures was done by densitrometric analysis of band intensities on Southern-hybridized total DNAs (*SI Text*). All time points represent those after culture inoculation, whereby 24 h corresponds to early stationary phase. RNA was isolated from stationary phase cultures of *P. knackmussii* strain B13 grown on MM with 10 mM 3CBA for 48 h at 30 °C, as described in ref. 21. The 5′ end of the transcript including *inrR* was mapped with the SMART RACE cDNA Amplification Kit (Clontech) according to the manufacturer's protocol (*SI Text*, Table S2.

Statistical Testing. Significance of different treatments (e.g., wild-type versus *inrR* mutant behavior) was examined by pairwise *t* test (two-sided, $P < 0.01$). Error bars denote standard deviations from the mean or calculated 95% confidence intervals in triplicate experiments.

ACKNOWLEDGMENTS. We thank Itzel Ramos and Dianne Newman for the gift of the *echerry* gene; Ted Farmer, David Johnsson and Thomas Nyström for discussion and for critical reading the manuscript. This work was supported by grants from the Swiss National Science Foundation (3100-67229, 3100A0-108199).

1. Ochman H, Lawrence JG, Groisman EA (2000) Lateral gene transfer and the nature of bacterial innovation. *Nature* 405:299–304.
2. Dobrindt U, Hochhut B, Hentschel U, Hacker J (2004) Genomic islands in pathogenic and environmental microorganisms. *Nat Rev Microbiol* 2:414–424.
3. Thomas CM, Nielsen KM (2005) Mechanisms of, and barriers to, horizontal gene transfer between bacteria. *Nat Rev Microbiol* 3:711–721.
4. Frost LS, Leplae R, Summers AO, Toussaint A (2005) Mobile genetic elements: The agents of open source evolution. *Nat Rev Microbiol* 3:722–732.
5. Vernikos GS, Parkhill J (2008) Resolving the structural features of genomic islands: A machine learning approach. *Genome Res* 18:331–342.
6. Greub G, Collyn F, Guy L, Roten CA (2004) A genomic island present along the bacterial chromosome of the *Parachlamydiaceae* UWE25, an obligate amoebal endosymbiont, encodes a potentially functional F-like conjugative DNA transfer system. *BMC Microbiol* 4:48.
7. He JX, *et al.* (2004) The broad host range pathogen *Pseudomonas aeruginosa* strain PA14 carries two pathogenicity islands harboring plant and animal virulence genes. *Proc Natl Acad Sci USA* 101:2530–2535.
8. Hsiao WW, *et al.* (2005) Evidence of a large novel gene pool associated with prokaryotic genomic islands. *PLoS Genet* 1:e62.
9. Klockgether J, Würdemann D, Reva O, Wiehlmann L, Tümmler B (2007) Diversity of the abundant pKLC102/PAGI-2 family of genomic islands in *Pseudomonas aeruginosa*. *J Bacteriol* 189:2443–2459.
10. Paulsen IT, *et al.* (2005) Complete genome sequence of the plant commensal *Pseudomonas fluorescens* Pf-5. *Nat Biotechnol* 23:873–878.
11. Perna NT, *et al.* (2001) Genome sequence of enterohaemorrhagic *Escherichia coli* O157:H7. *Nature* 409:529–533.
12. Simpson AJ, *et al.* (2000) The genome sequence of the plant pathogen *Xylella fastidiosa*. *Nature* 406:151–157.
13. Mathee K, *et al.* (2008) Dynamics of *Pseudomonas aeruginosa* genome evolution. *Proc Natl Acad Sci USA* 105:3100–3105.
14. Coburn PS, Baghdayan AS, Dolan GT, Shankar N (2007) Horizontal transfer of virulence genes encoded on the *Enterococcus faecalis* pathogenicity island. *Mol Microbiol* 63:530–544.
15. Ubeda C, Barry P, Penades JR, Novick RP (2007) A pathogenicity island replicon in *Staphylococcus aureus* replicates as an unstable plasmid. *Proc Natl Acad Sci USA* 104:14182–14188.
16. Dobrindt U, *et al.* (2003) Analysis of genome plasticity in pathogenic and commensal *Escherichia coli* isolates by use of DNA arrays. *J Bacteriol* 185:1831–1840.

17. Larbig K, *et al.* (2002) Gene islands integrated into $tRNA^{Gly}$ genes confer genome diversity on a *Pseudomonas aeruginosa* clone. *J Bacteriol* 184:6665–6680.
18. Buchrieser C, Prentice M, Carniel E (1998) The 102-kilobase unstable region of *Yersinia pestis* comprises a high- pathogenicity island linked to a pigmentation segment which undergoes internal rearrangement. *J Bacteriol* 180:2321–2329.
19. Beaber JW, Hochhut B, Waldor MK (2002) Genomic and functional analyses of SXT, an integrating antibiotic resistance gene transfer element derived from *Vibrio cholerae*. *J Bacteriol* 184:4259–4269.
20. Mohd-Zain Z, *et al.* (2004) Transferable antibiotic resistance elements in *Haemophilus influenzae* share a common evolutionary origin with a diverse family of syntenic genomic islands. *J Bacteriol* 186:8114–8122.
21. Gaillard M, *et al.* (2006) The clc element of *Pseudomonas* sp. strain B13, a genomic island with various catabolic properties. *J Bacteriol* 188:1999–2013.
22. Toussaint A, *et al.* (2003) The biphenyl- and 4-chlorobiphenyl-catabolic transposon Tn4371, a member of a new family of genomic islands related to IncP and Ti plasmids. *Appl Environ Microbiol* 69:4837–4845.
23. Sullivan JT, *et al.* (2002) Comparative sequence analysis of the symbiosis island of *Mesorhizobium loti* strain R7A. *J Bacteriol* 184:3086–3095.
24. Sørensen SJ, Bailey M, Hansen LH, Kroer N, Wuertz S (2005) Studying plasmid horizontal transfer in situ: A critical review. *Nat Rev Microbiol* 3:700–710.
25. Dubnau D, Losick R (2006) Bistability in bacteria. *Mol Microbiol* 61:564–572.
26. Smits WK, Kuipers OP, Veening JW (2006) Phenotypic variation in bacteria: The role of feedback regulation. *Nat Rev Microbiol* 4:259–271.
27. Beaber JW, Hochhut B, Waldor MK (2004) SOS response promotes horizontal dissemination of antibiotic resistance genes. *Nature* 427:72–74.
28. Juhas M, *et al.* (2007) Novel type IV secretion system involved in propagation of genomic islands. *J Bacteriol* 189:761–771.
29. Qiu X, Gurkar AU, Lory S (2006) Interstrain transfer of the large pathogenicity island (PAPI-1) of *Pseudomonas aeruginosa*. *Proc Natl Acad Sci USA* 103:19830–19835.
30. Ramsay JP, Sullivan JT, Stuart GS, Lamont IL, Ronson CW (2006) Excision and transfer of the *Mesorhizobium loti* R7A symbiosis island requires an integrase IntS, a novel recombination directionality factor RdfS, and a putative relaxase RlxS. *Mol Microbiol* 62:723–734.
31. Sentchilo VS, Ravatn R, Werlen C, Zehnder AJB, van der Meer JR (2003) Unusual integrase gene expression on the clc genomic island of *Pseudomonas* sp. strain B13. *J Bacteriol* 185:4530–4538.
32. Ravatn R, Studer S, Zehnder AJB, van der Meer JR (1998) Int-B13, an unusual site-specific recombinase of the bacteriophage P4 integrase family, is responsible for chromosomal insertion of the 105-kilobase clc element of *Pseudomonas* sp. strain B13. *J Bacteriol* 180:5505–5514.
33. Burrus V, Waldor MK (2004) Shaping bacterial genomes with integrative and conjugative elements. *Res Microbiol* 155:376–386.
34. Ravatn R, Zehnder AJB, van der Meer JR (1998) Low-frequency horizontal transfer of an element containing the chlorocatechol degradation genes from *Pseudomonas* sp. strain B13 to *Pseudomonas putida* F1 and to indigenous bacteria in laboratory-scale activated-sludge microcosms. *Appl Environ Microbiol* 64:2126–2132.
35. Sentchilo VS, Zehnder AJB, van der Meer JR (2003) Characterization of two alternative promoters and a transcription regulator for integrase expression in the clc catabolic genomic island of Pseudomonas sp. strain B13. *Mol Microbiol* 49:93–104.
36. Shaner NC, *et al.* (2004) Improved monomeric red, orange and yellow fluorescent proteins derived from *Discosoma* sp. red fluorescent protein. *Nat Biotechnol* 22:1567–1572.
37. Losick R, Desplan C (2008) Stochasticity and cell fate. *Science* 320:65–68.
38. Gaillard M, Pernet N, Vogne C, Hagenbüchle O, van der Meer JR (2008) Host and invader impact of transfer of the clc genomic island into *Pseudomonas aeruginosa* PAO1. *Proc Natl Acad Sci USA* 105:7058–7063.
39. Becker G, Hengge-Aronis R (2001) What makes an *Escherichia coli* promoter σ^S dependent? Role of the -13/-14 nucleotide promoter positions and region 2.5 of σ^S. *Mol Microbiol* 39:1153–1165.